Exploring the impact of Verticillium wilt disease on the mechanical properties of elementary flax (Linum usitatissimum L.) fibres

Lucile Nuez, Sylvie Durand, Alessia Melelli, Jean-Guy Berrin, Mireille Haon, Elodie Drula, Johnny Beaugrand, Pierre D'arras, Alain Bourmaud, Christophe Baley

Exploring the impact of verticillium wilt disease on the mechanical properties of elementary flax (*Linum usitatissimum* L.) fibres

Lucile Nuez [a, b] ; Sylvie Durand [c] ; Alessia Melelli [a] ; Jean-Guy Berrin [d]; Mireille Haon [d]; Elodie Drula [d,e,f]; Johnny Beaugrand [c] ; Pierre D'Arras [b] ; Alain Bourmaud [a] ; Christophe Baley [a]

a : Univ. Bretagne Sud, UMR CNRS 6027, IRDL, F-56100 Lorient, France

b: Van Robaeys Frères, 83 Rue Saint-Michel, 59122 Killem, France

c: Biopolymères Intéractions Assemblages (BIA), INRAE, Rue de la Géraudière, F-44316 Nantes, France

d : INRAE, Aix Marseille Univ., UMR1163 Biodiversité et Biotechnologie Fongiques, F13009 Marseille, France

e : INRAE, USC1408, AFMB, F13009 Marseille, France

f : CNRS, Aix Marseille Univ, UMR7257, AFMB, F13009 Marseille, France

* Corresponding author: alain.bourmaud@univ-ubs.fr; Tel.: +33-2-97-87-45-18

Abstract

Verticillium wilt is a disease caused by the fungus *Verticillium dahliae* (*V. dahliae*) which is widespread in flax (*Linum usitatissimum L.*) cultures. *V. dahliae* negatively impacts the fibre yield with up to 60 % loss at the scutching step of fibre transformation. Yet, little is known

about the consequences of *V. dahliae* on the mechanical properties of flax fibres. In this study, we investigated the tensile characterisation of elementary flax fibres impacted by *V. dahlia*. Using elementary tensile tests, we observed an important decrease in the mechanical properties of the studied flax fibres, with a 32 % decrease of the tensile strength at break and a 15 % decrease of the strain at break. Further investigation of the flax fibres cell wall using atomic force microscopy (AFM) in peak-force non-quantitative mechanical mapping mode, showed a 23 % decrease in the longitudinal indentation modulus of flax fibre cell walls, measured directly in their cross section. This is arguably due to the important enzymatic arsenal of *V. dahliae* revealed by a bioinformatic analysis of secreted carbohydrate-active enzymes targeting plant cell wall components. The coupling of this analysis with electron microscopy observations and sugar analysis highlighted the degradation mechanisms of this fungus which significantly affects the mechanical performance of flax fibres.

Keywords: AFM PF-QNM; carbohydrate-active enzymes*;* elementary fibre; *Linum usitatissimum L.*; tensile properties*; Verticillium dahliae*

1. Introduction

Environmental concerns encourage the use of flax fibres (*Linum usitatissimum L.*) for both technical and textile applications as a result of their outstanding tensile mechanical properties and limited environmental impact (Baley & Bourmaud, 2014; Le Duigou et al., 2011). Flax fibres are made up of multi-layered cell walls, but weather conditions directly affect the growth of flax, in particular during the filling of the elementary fibres (Goudenhooft et al., 2018). Hydric stress delays the formation of flax fibres, specifically during the elongation phase

(Chemikosova et al., 2006). This results in shortened fibres and altered cell wall formation due to a change in biochemical composition (Chemikosova et al., 2006), and more globally results in shorter flax stems (Kariuki et al., 2016) that negatively impact the fibre production during the scutching process.

Verticillium dahliae (*V. dahliae*) is a pathogen that causes the Verticillium wilt disease to flax stems. *V. dahliae* is found at the stage of dormancy in the soil as microsclerotia, that consists of a compact cluster of mycelium, which can confer more than 14 years survival to the fungus (Bressan et al., 2016). *V. dahliae* is extremely polyphagous with more than 200 potential host species including potato and salad (Bressan et al., 2016; Mol, 1995). Fungal growth is stimulated by an increase in temperature and humidity in the soil, in particular by root exudate (Blum et al., 2018; Valade et al., 2019), but climate change may also encourage the germination of *V. dahliae*.

This vascular fungus penetrates by the roots of flax at an early stage of growth (vegetative stage) when the stems are approximately 10 cm high (Goudenhooft et al., 2019). *V. dahliae* then progresses acropetally inside the conducting vessels of the xylem with raw sap. This environment is relatively poor in polysaccharides or mineral resources (Klosterman et al., 2011). Yet, the evolution of *V. dahliae* in this environment prevents it from having to compete with other microorganisms present in the different tissues of the plant (Yadeta & Thomma, 2013). Blum et al. (2018) have carried out inoculation test with *V. dahliae* during hydroponic cultivation of flax by dipping the stems in a solution containing conidia (spores produced by *V. dahliae*). After one week post inoculation (wpi), the cell differentiation zone was completely colonized by *V. dahliae* and most of hyphae were oriented parallel to the longitudinal axis of the roots. Located at the intercellular junction, the hyphae developed several swollen structures similar to appressoria that allow the fungus to penetrate into a host cell. The entry

of *V. dahliae* into the xylem causes a series of defence reactions from the plant, such as by the formation of tyloses, pectin gels or gums, phenolic compounds or inorganic sulfur (Blum et al., 2018). Leaves wilting appeared approximately three to four wpi and at eight wpi the fibre bundles were not yet reached by *V. dahliae*. The presence of mycelium in the primary superficial tissue cells of flax roots was also noted by Marchal (Marchal, 1940). These filaments formed chalydospores, which are disposed in small chains or gathered into bunches to constitute microsclerotia.

The systematic development of *V. dahliae* causes the wilting of the plant due to a disturbance of the flow of raw sap in the xylem. Nevertheless, the first symptoms, which also include a wilting of the leaves starting at the base of the stem, and a chlorose (discoloration) of the stem are not sufficient to establish a reliable diagnostic at this stage because these symptoms are very similar to that caused by hydric stress of other fungal pathogens such as *Fusarium* spp. (Blum et al., 2018). The symptoms are more distinctive at the flower stage of flax and especially during retting, with a metallic blue coloration of the stems and easily separable fibre bundles from the woody core of the stem. *V. dahliae* can cause up to a 60 % loss in long fibre yield at the scutching step of fibre transformation, and consequently an important production of flax tows (Arvalis, 2019). Thus, the decrease in long fibre yield is due to the fibre breakage induced by the disease but the number of single fibres in the plant does not really change, the main difference is the change in fibre morphology, inducing a large number of short fibres, i.e flax tows.

The control of the development of *V. dahliae* is particularly difficult because of its important persistence in the soil (Bressan et al., 2016), and also because of its polyphagia (Mol, 1995). There are currently only very few resistant plant species and none of them concern fibre flax. Rotational cultures (every 6 or 7 years regarding flax) are therefore necessary with the

92 introduction of non-host or resistant species between the cultivation of at-risk species in order
93 to limit the development of pathogens such as verticillium wilt. There are currently no
94 fungicides nor biocontrol of seeds, vegetation or soil. Other advices include the management
95 of cultural residues, in particular by exporting the straws from the fields (which is already the
96 case for fibre flax) and the cleaning of the harvest material to avoid the contamination of
97 neighbouring parcels (Valade et al., 2019). New detection methods based on DNA analysis
98 allowed to quantify and to establish maps of the infected field zone. Knowledge of the density
99 of *V. dahliae* in a parcel before sowing can also be an interesting way to protect future cultures
100 (Bressan et al., 2016).

101 The consequences of *V. dahlia* on flax fibre yields are important, but its impact at the scale of
102 elementary fibres is still unknown. Its consequences for a use in technical applications, for
103 example as biocomposite reinforcement material and textile, is, to the best of our knowledge,
104 unexplored. This study aims at the mechanical characterization of elementary fibres of a flax
105 sample infected by *V. dahliae* on fibre bundles to understand its evolution. This investigation
106 was further completed, at the cell wall scale, with measures by atomic force microscopy (AFM)
107 in peak-force quantitative nanomechanical mapping mode. Scanning electron microscopy
108 observations, bioinformatic genomic assessment and biochemical assessment were also used
109 to better explain the impacts of *V. dahliae* on the mechanical properties of flax at the scale of
110 cell walls and of elementary fibres.

111

2. Materials and Methods

2.1. Flax fibres and bundles

A sample of reference long scutched flax (*Linum usitatissimum L.*) fibres from the Avian variety was provided by Van Robaeys Frères (France). It was cultivated in 2017 in France in the Picardy region and corresponds to a good quality sample regarding a use in the textile field. A sample of fibres of the same variety cultivated in 2020 also in the Picardy region, and impacted by *V. dahlia* was studied in comparison. For these two cultivation years, the cumulative rain fall and mean temperatures as well as mean maximum and minimum temperatures were analogous.

The two batches were dew-retted for approximatively 6 weeks. The level of infection was not quantified but corresponds to the infection present on the stems following retting. The elementary fibres and fibre bundles were extracted by hand from the median part of the stems. Only the fibres from the middle of the stem were studied.

2.2. Molecular authentication (DNA extraction, PCR, and sequencing).

Approximately 100 mg of mycelium present at the surface of infected flax samples (Fig.1.a) was scraped and genomic DNA was extracted using the NucleoSpin PlantII Kit (Macherey–Nagel, France). The ribosomal DNA internal transcribed spacer region (rDNA-ITS) was then amplified by PCR using the ITS5/ITS4 primers as described in (Navarro et al., 2021) DNA amplification was performed in a Mastercycler Nexus GSX1 (Eppendorf, Montesson, France) and the PCR product was sequenced by Genewiz (Leipzig, Germany). The sequence was compared with sequences in the GenBank database using blastn.

2.3. Scanning electron microscopy (SEM) observations

The flax fibres and bundles were observed using a Jeol JSM 6460LV (France) scanning electron microscope (SEM). Each sample was first sputter coated with a thin layer of gold (Edwards Sputter Coater, France) in high vacuum to avoid them from charging during analysis.

2.4. Tensile testing of elementary fibres

The flax fibres were extracted by hand and glued to paper frames with a gauge length of 10 mm. Their diameter was then measured by optical microscopy (Olympus AX70) at six positions along each fibre and the cross-sectional area was calculated from the mean measured diameter. The tensile tests were carried out using an MTS machine (France) with a 2 N force sensor and a tensile speed of 1 mm/min. The compliance of the set-up was measured and used for the calculation of the strain and tangent modulus according to the NF T25-501-3 standard. The latter was measured from the last linear zone of the stress strain curve of each fibre, in agreement with the NF T 501-2 standard.

2.5. Atomic force microscopy (AFM)

The longitudinal indentation modulus of the flax cell walls (measured on fibre cross section) was investigated by atomic force microscopy (AFM, Bruker, USA) in peak force quantitative nanomechanical mapping mode (PF-QNM). Flax fibres bundles were first cut in 10 mm segments and glued upon 5 mm long paper frames. The embedding protocol is precisely described in (Goudenhooft et al., 2018). Transversal sections of the samples were obtained with an ultramicrotome (Leica Ultracut R) equipped with diamond knives (Diamond Histo and

156 Ultra AFM). The indentation modulus of the cell walls was measured with a specific tip with a
157 stiffness constant of 139 N/m, a tip radius between 15 and 35 nm, a scan frequency of 8 µm/s
158 and a maximum force of 200 N were used for the measures. The tip and probe cantilever
159 calibration protocol is described by Arnould et al. (Arnould et al., 2017). In order to control the
160 AFM measurements, the indentation modulus of several positions across the thickness of the
161 G cell wall layer but also of the embedding resin were measured by nanoindentation prior to
162 AFM measurements. Image treatment was carried out using the Gwyddion software (Nečas &
163 Klapetek, 2012).

164

165 **2.6. Biochemical composition analysis**

166 Wet chemical analysis was used to evaluate the monosaccharide content of both the reference
167 and the verticillium infected fibres. First, sample homogenization was carried out by
168 cryogrinding approximately 1g of each flax fibre bundles samples (SPEX 6700 freezer Mill). The
169 latter were then hydrolysed in 12 M H2SO4 (Sigma Aldrich) for 2 h maintained at 25 °C by a
170 heating plate, then an additional hydrolysis was carried out during 2 h at 100 °C with 1.5 M
171 H2S04 in which inositol was used as internal standard. Individual neutral monosaccharides
172 (arabinose, rhamnose, fucose, glucose, xylose, galactose and mannose) were analysed as their
173 alditol acetate derivatives (Blakeney et al., 1983) by gas-liquid chromatography (Perkin Elmer,
174 Clarus 580, Shelton, CT, USA) equipped with an DB 225 capillary column (J&W Scientific,
175 Folsorn, CA, USA) at 205°C, with H2 as the carrier gas. Furthermore, Galacturonic Acid (GalA)
176 and Glucuronic Acid (GlcA) were determined by an automated m-hydroxybiphenyl method
177 (Thibault, 1979) and merged as Uronic acid (UrAc). Standards of carbohydrate solutions with
178 three known concentrations were used for calibration. Analyses were performed in three

179 independent assays. The total monosaccharide content is the sum of each monosaccharide
180 amount, and is expressed as the percentage of the dry matter mass.

181 The lignin content was quantified by colorimetric analysis for each sample in triplicates
182 subsequently to the acetyl bromide method (Hatfield & Fukushima, 2005). Sample mass was
183 approximately 20 mg per essay, the chemicals used were laboratory grade from Sigma Aldrich,
184 and the lignin content is reported as the percentage of the dry matter mass.

185

186 **2.7. Analysis of *V. dahlia* genome for secreted carbohydrate-active enzymes**

187 All putative proteins of *Verticillium dahlia* genome (Klosterman et al., 2011) were compared to
188 the entries in the CAZy database (Drula et al., 2022). A homemade pipeline which combines
189 BlastP (https://blast.ncbi.nlm.nih.gov/Blast.cgi) and HMMER3 (http://hmmer.janelia.org/)
190 tools was used to compare protein models with the sequences of the CAZy modules. The
191 proteins with E-values smaller than 0.1 were further screened by a combination of BlastP
192 searches against libraries created from the sequences of the catalytic and non-catalytic
193 modules. HMMER3 was used to query against a collection of custom-made hidden Markov
194 model (HMM) profiles constructed for each CAZy family. This was followed by a manual
195 inspection by expert curators to resolve borderline cases. Peptide signals were predicted using
196 Phobins (Käll et al., 2004).

197

198

3. Results and Discussion

3.1. SEM observations

The presence of the fungal pathogen was confirmed on infected flax samples using the barcoding ITS gene. After DNA extraction and sequencing, the best match was *V. dahliae* with high confidence (more than 99% sequence identity). We also evaluated the presence of *V. dahliae* with SEM observations of the infected flax sample as compared to reference flax fibres (**Figure 1)**. It is possible to notice that the reference flax fibre bundles are comparatively clean with little organic residues at their surface. The fibres are individualised and reasonably accessible, as shown in **Figure 1**b and d. However, the fibres of flax infected by *V. dahliae* fibres display many microsclerotia at the surface of the bundles (**Figure 1**c, e), and fungal filaments which correspond to *V. dahlia* mycelium (Marchal, 1940). These microsclerotia are clinging to the cell walls and colonize the flax bundles continuously along their length.

Figure 1

V. dahliae develops in the flax xylem during its growth and progresses acropetally with the raw sap towards the plant's apex. Studies of incubation have shown that this progression is performed during several weeks and that after 8 wpi, *V. dahliae* had not yet reached the fibres situated at the periphery of the stem (Blum et al., 2018), the authors suggested that fibre degradation could take place when the stem is unable to defend itself anymore. The growing of flax takes place during 12 to 16 weeks, and it is possible that the fibre infection takes place before their maturity, but also following stem pull-out and during the retting phase. From

these images, it is not possible to know at which growth stage the fibres were colonized by *V. dahliae*, but the microsclerotia are extremely present following sample retting and storing.

Figure 2.

Figure 2 shows the visual longitudinal aspect of an elementary fibre infected by *V. dahlia* observed by SEM. Examination reveals microcracks that are visible lengthwise. Such defects are not present on the reference elementary flax fibres. Furthermore, the infected fibres show an important surface roughness, resulting from concomitant mechanical and enzymatic degradation mechanisms caused by *V. dahliae.*

3.2. Tensile mechanical properties of the elementary flax fibres

The results of the tensile tests are given in **Table 1** for both the reference flax fibres and the *V. dahliae* sample. A clear decrease is noticeable in the mechanical properties for the latter contaminated sample. The tangent modulus of the colonized fibres shows a -20 % reduction compared to the reference sample, for which the modulus is measured at 43.6 ± 17.0 GPa. Despite a value that is located in the lower standard deviation of the mean tangent modulus measured at 52.5 ± 8.5 GPa from testing 50 different flax fibre batches (Baley & Bourmaud, 2014), the measured modulus is in agreement with the literature. Furthermore, a Mann-Whitney statistical nonparametric test was carried out on the two populations and confirms that the two populations are significantly different with a significant level of 0.05.

243 **Table 1**

244

245 The infection by *V. dahliae* also causes an important decline in the tensile strength at break of
246 the elementary fibres, measured at 773 ± 374 MPa for the reference sample, against 522 ± 322
247 MPa for the *V. dahliae* sample, which represents a -32 % relative difference. Finally, the strain
248 at break of the elementary fibres is also affected, with a -15 % decrease measured for the *V.*
249 *dahliae* sample compared to the reference sample, at 1.78 ± 0.69 % and 2.09 ± 0.59 %
250 respectively. A Mann-Whitney statistical test also confirms for both the strength and the strain
251 at break that the reference and Verticillium wilt fibre samples are significantly different.

252 Lefeuvre at al. (Lefeuvre, Bourmaud, et al., 2015) have shown the importance of the fibre
253 sampling zone on their cross section area and tensile mechanical properties. Furthermore, a
254 correlation has been observed between the tangent modulus of flax fibres and their measured
255 diameter before tensile testing (Charlet et al., 2009). Yet, the diameter of the flax fibres from
256 the two tensile-tested samples is similar at 15.23 ± 3.13 µm and 16.21 ± 3.39 µm for the
257 reference and the *V. dahliae* sample, respectively, suggesting the representative results.

258 **Figure 3** allows a comparison of the cumulative probability of the strength at break of both the
259 reference and the *V. dahliae* sample. The figure brings in light that 80 % of the fibres affected
260 by *V. dahliae* have a strength at break at 650 MPa, whereas this corresponds to that of 50 % of
261 the reference sample. The first and third quartile of the *V. dahliae* sample are at approximately
262 200 and 600 MPa, against 366 and 968 MPa for the reference flax fibres.

263

264 **Figure 3**

The damages visible on the outer surface and cross-section of the fibres following *V. dahliae* (**Figure 2**), partly explain the loss of strength at break for this sample. The irregular section causes localised zones of strain concentration during the tensile tests. The strength at break is highly dependent on the presence of microscopic defects according to the Griffith theory (Griffith, 1921). These damages lead also to an overestimation of the real cross section of fibres at their rupture location, and therefore an underestimation of the strength at break and the tangent modulus. But because of the visual aspect of the transversal cross-section (**Figure 4.b**) and of the negligible difference between the diameters of the fibres from both samples, the comparison of the range of their mechanical properties is possible. Nevertheless, the defects caused by *V. dahliae*, such as the ones shown in **Figure 2**, induce localized strain concentrations during tensile testing, which may create local damages at the origin of the rupture initiation of the fibre (**Table 1**). It is also possible that defect zones like kink-bands are possible sensitive zones to the action of enzymes (Thygesen et al., 2011), slightly decreasing the strength at break of the fibres during tensile tests.

The mechanical properties given in **Table 1** highlight the decrease in the tangent modulus. A modification in the cellulose and pectin content in the cell walls can explain this phenomenon, as well as the difference in the measured strength at break between both samples of the study (**Figure 3**) (Lefeuvre, Le Duigou, et al., 2015). Crystalline cellulose is indeed the major polysaccharide responsible for the mechanical properties of plant cell walls. It is present in the form of microfibrils well-ordered with a small helical angle with regards to the fibre axis in the S2-G layer of flax fibres. The cellulases and pectinases secreted by *V. dahliae* can modify the microstructure of the cell walls, and hypothetically impact the behaviour of the microfibrils during a tensile test. A lower amount of pectin combined with a modification of the internal

289 organisation of the cell walls in particular with the appearance of important defects can also
290 decrease the load transfer between the cellulose microfibrils. In the literature, it is reported
291 that a reduction of approximately 10 % in weight of non-structural polysaccharides content
292 leads to a reduction by a factor 2 of the shear strength necessary to initiate the reorientation
293 of the cellulose microfibrils in the cell walls of elementary flax fibres (Lefeuvre, Le Duigou, et
294 al., 2015). Despite the important loss of tangent modulus and strength at break observed for
295 the verticillium wilt sample with regard to the reference sample (**Table 1**), these elementary
296 fibres have sufficient mechanical properties to be used as composite materials reinforcements.

297

298 **3.3. Longitudinal modulus of the cell walls measured by nanoindentation**

299 To quantify the evolution of the stiffness of cell walls of flax fibres, AFM analyses were carried
300 out by means of a longitudinal solicitation in the transverse section of fibre bundles. **Figure 4**a
301 and b show a cartography of the indentation modulus of the cell walls of respectively the
302 reference and Verticillium wilt flax fibres obtained by the peak-force quantitative
303 nanomechanical mapping imaging mode. **Figure 4**c presents the distribution of the indentation
304 modulus of both sample but from the different observation zones. The mean indentation
305 modulus of the reference sample is 20.39 ± 3.54 GPa against 15.72 ± 2.61 GPa for the *V.*
306 *dahliae* sample, which represents a relative decrease of -23 %.

307

308 **Figure 4**

309

310 The modulus of indentation obtained by AFM for the reference fibres is coherent with the
311 values of the literature, between 18 and 24 GPa (Goudenhooft et al., 2018)(Marchal,
312 1940)(Nečas & Klapetek, 2012)(Blakeney et al., 1983). Despite the dependence of sample
313 preparation and in particular to the stiffness of the embedding resin and the geometry of the
314 tip used for the AFM measurements, the values obtained here are coherent for mature and
315 healthy flax fibres.

316 In **Figure 4**b, the local indentation modulus of the fibres from the *V. dahliae* sample is shown.
317 Unlike the reference sample, the fibres have an irregular cross-section and degraded cell walls.
318 These irregularities are located at the outer periphery of the cells and sometimes reach the
319 lumen, as visible in the detailed view of **Figure 5**a. The indentation modulus distribution profile
320 along the white arrow of **Figure 5**a, as shown in **Figure 5**b, highlights a relatively constant
321 stiffness at approximately 16 GPa throughout the cell wall surface, with a slight decrease of the
322 stiffness at the external periphery of the fibres. The lumen is visible at a distance of 3.8 µm
323 along the plotted profile, and another internal porosity seems to be present at a distance of 2
324 µm. These additional internal porosities have in fact been measured in elementary fibres in the
325 literature by (Richely et al., 2021).

326

327 **Figure 5**

328

329 *V. dahliae* can release numerous enzymes during the vascular infection of a plant, in particular
330 cellulases and a multitude of pectin degrading enzymes. These enzymes are particularly well
331 adapted to the environment in which *V. dahliae* evolves, specifically in the xylem fluids where
332 the concentration in carbohydrates, amino acids and inorganic ions is weak (Klosterman et al.,

2011). The *V. dahliae* genome contains an important number of polysaccharide lyases and rhamnogalacturonan lyases (Klosterman et al., 2011). This diversity of enzymes illustrated the capacity of *V. dahliae* to degrade cell walls and allows *V. dahliae* to progress inside the vessels of the xylem. The degraded surface aspect of the elementary fibres is a consequence of the colonization of *V. dahliae*. Particularly, the pectinases and cellulases produced by *V. dahliae* can be at the origin of the important decrease in local stiffness of the cell walls measured by AFM due to a possible reduction of cellulose crystallinity. Local stiffness is indeed dependent on the cellulose content and on the chemical composition of the cell walls (Gindl et al., 2002; Gindl et al., 2004). The influence of pectin on the mechanical behaviour of elementary fibres has been investigated by Lefeuvre et al. (Lefeuvre, Le Duigou, et al., 2015). The extraction of polysaccharides presents in the amorphous matrix of the cell walls, notably in the pectin matrix, leads to a -30 % drop in the tensile strength at break of the fibres. A -29 % drop in the modulus of fibres has also been shown following the extraction of structural polysaccharides.

Figure 6

The cell wall degradation of the *V. dahliae* sample fibres is also confirmed by SEM observations, shown in **Figure 6**. The fibres are mainly degraded at their periphery but also locally towards the centre of the lumen. The reference flax fibre bundles show in contrast the expected mature polygonal cell walls with a very small lumen here.

3.4. Biochemical composition

Table 2 shows the results of the biochemical composition analysis carried out on fibres bundles of the reference and verticillium wilt flax sample. The hemicelluloses composition is overall very similar. A 22 % and a 38 % relative increase in mannose and xylose respectively for the *V. dahliae* fibre sample compared to the reference fibres can be noted. There is also a 28 % relative difference between the lignin content of the reference and the Verticillium wilt sample, but no significant difference in the amount of glucose between the two samples.

Table 2

Studies have shown that *V. dahliae* possesses an important enzymatic arsenal containing an important and complex amount of polysaccharide lyases, including in particular pectate lyases and rhamnogalacturonan lyases (Klosterman et al., 2011). Klosterman et. al suggested that this allowed the pathogen to use the pectin in the plant cell walls or from the gels released in the xylem by plant infection reaction mechanisms. The pectin degrading enzymes may directly contribute the progression of the *V. dahliae* within the xylem vessels, and eventually allow it to reach the flax fibre bundles (Blum et al., 2018).

The slight differences in lignin and other polysaccharide contents can be attributed to inter-variety scatter or to soil and climate differences between the cultivation areas and times of the samples. This modest difference could possibly be due to a defence reaction from the plant (Paul-Victor et al., 2017) but the time of infection is not precisely known in the present study.

3.5. Genomic analysis of *V. dahliae* carbohydrate-active enzymes

To evaluate the degradation potential of *V. dahliae,* we performed annotation of its genome with a focus on enzymes targeting plant cell wall polysaccharides, *i.e.*, CAZymes predicted to degrade cellulose, hemicelluloses or pectin. Out of the 489 CAZymes predicted to be involved in polysaccharides catabolism, 311 CAZymes are predicted to be secreted, of which 172 are predicted to be involved in cellulose, hemicelluloses and pectin degradation. When focusing only on the plant cell wall degrading CAZymes secreted, we noticed that *V. dahliae* displays an impressive array of enzymes belonging to the different CAZy classes (GH, glycoside hydrolases; AA, auxiliary activity enzymes; CE, carbohydrate esteresases; PL, polysaccharide lyases) targeting the different component of plant cell wall (cellulose, hemicelluloses and pectin) (**Figure 7**).

Figure 7

As previously observed, *V. dahliae* is predicted to secrete 72 pectin-degrading enzymes including 38 polysaccharide lyases. Another interesting observation is the large array of lytic polysaccharide monooxygenases (LPMOs) with 26 enzymes from the families AA9 and AA16, predicted to be involved in the oxidative degradation of cellulose (Bennati-Granier et al., 2015; Filiatrault-Chastel et al., 2019) together with their redox partners (e.g., AA3-AA8 cellobiose dehydrogenase) required to trigger LPMO activity (**Table 3**). Interestingly, fungal LPMOs create nicking points that lead to the disruption of the cellulose fibre structure with rupture of chains (Villares et al., 2017). This bioinformatic analysis is in line with SEM and biochemical

assessment, supporting the high degradation potential of *V. dahliae*, being in capacity to simultaneously degrade major components of flax cell walls.

4. Conclusion

Flax fibres are sensitive to numerous diseases during its cultivation, in particular to the fungus *V. dahliae* that develops inside the vessels of the xylem of flax during growth of the plant. Even if *V. dahliae* is a vascular parasite, *V. dahliae* can reach the fibres bundles, especially following the stem pull out, and can cause important damages to the fibre yield during scutching. Its consequences on the mechanical properties of elementary fibres are also substantial, with a -20 % decrease in the fibre stiffness and a -32 % decrease in fibre strength for the studied sample. This could be explained by the local cell wall damages caused by the CAZymes secreted by *V. dahliae*, which may be at the origin of strain concentrations and therefore premature fibre failure.

They also affect the volume of the cell walls, causing a -25 % decrease in the indentation modulus measured by AFM for elementary flax fibres compared to reference fibres. We suggest that the pectinases and cellulases (especially the LPMOs) predicted to be secreted by *V. dahliae* could be at the origin of such a modification in the cell walls affected by *V. dahliae*. However, the development stage of *V. dahliae,* the origin of the flax sample (location of the fibres along the stem, growth conditions, etc.) are all factors that must be taken into account when considering the mechanical property evolution of the fibres. Future work perspectives concern a possible progression of the Verticillium wilt disease from the xylem of the flax stem to the peripheral fibre bundles, but also a hypothetical evolution of the pathogen on the fibres

during their storage and use. In this objective, a hydroponic/root dipping method for plant cultivation and inoculation, and green fluorescent protein modified strains could be carried out to follow the *in-planta* development of *V. dahliae* at lab scale.

Without a preventive solution other than crop rotation in fields, the consequences of this disease, from which the symptoms are difficult to detect with certainty during the growth of flax stems, are significant. This is alarming regarding the yields at the different processing steps of flax fibres as *V. dahliae* can already cause up to a -60 % loss in fibre yields at the scutching step, and has important consequences on the mechanical properties of flax fibres as reinforcement of biocomposites or textiles.

Acknowledgements

The authors would like to thank the National Association of Research and Technology for funding Lucile Nuez's thesis in partnership with Van Robaeys Frères and the Dupuy de Lôme Research Institute of the Université de Bretagne-Sud (France). They also sincerely thank Sylviane Daniel and Lucas Demezet (INRAE-BIA) for the technical support provided for biochemical experiments. The authors wish also to acknowledge the funding provided by the INTERREG IV Cross Channel programme through the FLOWER project (Grant Number 23).

References

Arnould, O., Siniscalco, D., Bourmaud, A., Le Duigou, A., & Baley, C. (2017). Better insight into the nano-mechanical properties of flax fibre cell walls. *Industrial Crops and Products*, *97*,

224–228. https://doi.org/10.1016/j.indcrop.2016.12.020

Arvalis. (2019). Culture du lin fibre : La production s'adaptera au changement climatique. *Perspectives Agricoles*, *468*, 8–11.

Baley, C., & Bourmaud, A. (2014). Average tensile properties of French elementary flax fibers. *Materials Letters*, *122*, 159–161. https://doi.org/10.1016/j.matlet.2014.02.030

Bennati-Granier, C., Garajova, S., Champion, C., Grisel, S., Haon, M., Zhou, S., Fanuel, M., Ropartz, D., Rogniaux, H., Gimbert, I., Record, E., & Berrin, J. G. (2015). Substrate specificity and regioselectivity of fungal AA9 lytic polysaccharide monooxygenases secreted by Podospora anserina. *Biotechnology for Biofuels*, *8*(1), 1–14. https://doi.org/10.1186/s13068-015-0274-3

Blakeney, A. B., Harris, P. J., Henry, R. J., & Stone, B. A. (1983). A simple and rapid preparation of alditol acetates for monosaccharide analysis. *Carbohydrate Research*, *113*(2), 291–299. https://doi.org/10.1016/0008-6215(83)88244-5

Blum, A., Bressan, M., Zahid, A., Trinsoutrot-Gattin, I., Driouich, A., & Laval, K. (2018). Verticillium Wilt on Fiber Flax: Symptoms and Pathogen Development In Planta. *Plant Disease*, *102*(12), 2421–2429. https://doi.org/10.1094/PDIS-01-18-0139-RE

Bressan, M., Blum, A., Castel, L., Trinsoutrot-Gattin, I., Laval, K., & Gangneux, C. (2016). Assessment of Verticillium flax inoculum in agroecosystem soils using real-time PCR assay. *Applied Soil Ecology*, *108*, 176–186. https://doi.org/10.1016/j.apsoil.2016.07.010

Charlet, K., Eve, S., Jernot, J. P., Gomina, M., & Breard, J. (2009). Tensile deformation of a flax fiber. *Procedia Engineering*, *1*(1), 233–236. https://doi.org/10.1016/j.proeng.2009.06.055

Chemikosova, S. B., Pavlencheva, N. V., Gur'yanov, O. P., & Gorshkova, T. A. (2006). The effect

of soil drought on the phloem fiber development in long-fiber flax. *Russian Journal of Plant Physiology*, *53*(5), 656–662. https://doi.org/10.1134/S1021443706050098

Drula, E., Garron, M.-L., Dogan, S., Lombard, V., Henrissat, B., & Terrapon, N. (2022). The carbohydrate-active enzyme database: functions and literature. *Nucleic Acids Research*, *50*(D1), D571–D577. https://doi.org/10.1093/nar/gkab1045

Filiatrault-Chastel, C., Navarro, D., Haon, M., Grisel, S., Herpoël-Gimbert, I., Chevret, D., Fanuel, M., Henrissat, B., Heiss-Blanquet, S., Margeot, A., & Berrin, J. G. (2019). AA16, a new lytic polysaccharide monooxygenase family identified in fungal secretomes. *Biotechnology for Biofuels*, *12*(1), 1–15. https://doi.org/10.1186/s13068-019-1394-y

Gindl, W., Gupta, H. S., & Grünwald, C. (2002). Lignification of spruce tracheid secondary cell walls related to longitudinal hardness and modulus of elasticity using nano-indentation. *Canadian Journal of Botany*, *80*(10), 1029–1033. https://doi.org/10.1139/b02-091

Gindl, W., Gupta, H. S., Schöberl, T., Lichtenegger, H. C., & Fratzl, P. (2004). Mechanical properties of spruce wood cell walls by nanoindentation. *Applied Physics A*, *79*(8), 2069–2073. https://doi.org/10.1007/s00339-004-2864-y

Goudenhooft, C., Bourmaud, A., & Baley, C. (2019). Flax (Linum usitatissimum L.) Fibers for Composite Reinforcement: Exploring the Link Between Plant Growth, Cell Walls Development, and Fiber Properties. *Frontiers in Plant Science*, *10*, 411. https://doi.org/10.3389/fpls.2019.00411

Goudenhooft, C., Siniscalco, D., Arnould, O., Bourmaud, A., Sire, O., Gorshkova, T., & Baley, C. (2018). Investigation of the mechanical properties of flax cell walls during plant development: The relation between performance and cell wall structure. *Fibers*, *6*(1).

https://doi.org/10.3390/fib6010006

Griffith, A. A. (1921). VI. The phenomena of rupture and flow in solids. *Philosophical Transactions of the Royal Society of London. Series A, Containing Papers of a Mathematical or Physical Character*, *221*(582–593), 163–198. https://doi.org/10.1098/rsta.1921.0006

Hatfield, R., & Fukushima, R. S. (2005). Can lignin be accurately measured? *Crop Science*, *45*(3), 832–839. https://doi.org/10.2135/cropsci2004.0238

Käll, L., Krogh, A., & Sonnhammer, E. L. L. (2004). A combined transmembrane topology and signal peptide prediction method. *Journal of Molecular Biology*, *338*(5), 1027–1036. https://doi.org/10.1016/j.jmb.2004.03.016

Kariuki, L. W., Masinde, P., Githiri, S., & Onyango, A. N. (2016). Effect of water stress on growth of three linseed (Linum usitatissimum L.) varieties. *SpringerPlus*, *5*(1), 759. https://doi.org/10.1186/s40064-016-2348-5

Klosterman, S. J., Subbarao, K. V., Kang, S., Veronese, P., Gold, S. E., Thomma, B. P. H. J., Chen, Z., Henrissat, B., Lee, Y. H., Park, J., Garcia-Pedrajas, M. D., Barbara, D. J., Anchieta, A., de Jonge, R., Santhanam, P., Maruthachalam, K., Atallah, Z., Amyotte, S. G., Paz, Z., … Ma, L. J. (2011). Comparative genomics yields insights into niche adaptation of plant vascular wilt pathogens. *PLoS Pathogens*, *7*(7). https://doi.org/10.1371/journal.ppat.1002137

Le Duigou, A., Davies, P., & Baley, C. (2011). Environmental impact analysis of the production of flax fibres to be used as composite material reinforcement. *Journal of Biobased Materials and Bioenergy*, *5*(1), 153–165. https://doi.org/10.1166/jbmb.2011.1116

Lefeuvre, A., Bourmaud, A., & Baley, C. (2015). Optimization of the mechanical performance of

509 UD flax/epoxy composites by selection of fibres along the stem. *Composites Part A:*
510 *Applied Science and Manufacturing*, *77*, 204–208.
511 https://doi.org/10.1016/j.compositesa.2015.07.009

512 Lefeuvre, A., Le Duigou, A., Bourmaud, A., Kervoelen, A., Morvan, C., & Baley, C. (2015).
513 Analysis of the role of the main constitutive polysaccharides in the flax fibre mechanical
514 behaviour. *Industrial Crops & Products*, *76*, 1039–1048.
515 https://doi.org/10.1016/j.indcrop.2015.07.062

516 Marchal, E. (1940). Observations et Recherches effectuées à la Station de Phytopathologie de
517 l'État pendant l'année 1939. *Bulletin de l'Institut Agronomique et Des Stations de*
518 *Recherches de Gembloux*, *9*(1–4), 1–15.

519 Mol, L. (1995). Formation of microsclerotia of Verticillium dahliae on various crops.
520 *Netherlands Journal of Agricultural Science*, *43*(2), 205–215.
521 https://doi.org/10.18174/njas.v43i2.577

522 Navarro D., Chaduli D., Taussac S., Lesage-Meesen L., Grisel S., Haon M., Callac P., Courtecuisse
523 R., Decock C., Dupont J., Richard-Forget F., Fournier J., Guinberteau J., Lechat C., Moreau
524 P-A., Pinson-Gadais L., Rivoire B., Sage L., Welti S., Rosso M-N., Berrin J-G., Bissaro B.,
525 Favel A. (2021). Large-scale phenotyping of 1,000 fungal strains for the degradation of
526 non-natural, industrial compounds. Communications Biology, 4, 871.
527 https://doi.org/10.1038/s42003-021-02401-w

528 Nečas, D., & Klapetek, P. (2012). Gwyddion: An open-source software for SPM data analysis.
529 *Central European Journal of Physics*, *10*(1), 181–188. https://doi.org/10.2478/s11534-
530 011-0096-2

Paul-Victor, C., Dalle Vacche, S., Sordo, F., Fink, S., Speck, T., Michaud, V., & Speck, O. (2017). Effect of mechanical damage and wound healing on the viscoelastic properties of stems of flax cultivars (Linum usitatissimum L. cv. Eden and cv. Drakkar). *PLoS ONE*, *12*(10), 1–23. https://doi.org/10.1371/journal.pone.0185958

Richely, E., Durand, S., Melelli, A., Kao, A., Magueresse, A., Dhakal, H., Gorshkova, T., Callebert, F., Bourmaud, A., Beaugrand, J., & Guessasma, S. (2021). Novel Insight into the Intricate Shape of Flax Fibre Lumen. *Fibers*, *9*(4), 24. https://doi.org/10.3390/fib9040024

Thibault, J. F. (1979). Automatisation du dosage des substances pectiques par la methode au meta-hydroxydiphenyl. In *Lebensmittel - Wissenschaft + Technologie. Food science + technology: Vol. v. 12*.

Thygesen, L. G., Hidayat, B. J., Johansen, K. S., & Felby, C. (2011). Role of supramolecular cellulose structures in enzymatic hydrolysis of plant cell walls. *Journal of Industrial Microbiology and Biotechnology*, *38*(8), 975–983. https://doi.org/10.1007/s10295-010-0870-y

Valade, R., Willaert, L., & Al., E. (2019). *La Verticilliose du lin Acquis et nouvelles perspectives pour une protection intégrée : La Verticilliose du lin causée par Verticillium dahliae*.

Villares, A., Moreau, C., Bennati-Granier, C., Garajova, S., Foucat, L., Falourd, X., Saake, B., Berrin, J. G., & Cathala, B. (2017). Lytic polysaccharide monooxygenases disrupt the cellulose fibers structure. *Scientific Reports*, *7*(September 2016), 1–9. https://doi.org/10.1038/srep40262

Yadeta, K. A., & Thomma, B. P. H. J. (2013). The xylem as battleground for plant hosts and vascular wilt pathogens. *Frontiers in Plant Science*, *4*(APR), 1–12.

https://doi.org/10.3389/fpls.2013.00097

Figure captions

Figure 1. Longitudinal SEM observations of *a) raw infected flax stems b*, *d*) the reference flax fibre sample, and of *c*, *e*) the V. dahliae flax fibre sample at different scales.

Figure 2. Longitudinal SEM observations of *V. dahliae* flax fibres showing a) microcracks in the cell wall and b) a rugous surface.

Figure 3. Cumulative probability of the strength at break of the reference and *V. dahliae* elementary flax fibre samples.

Figure 4. AFM measurements of a) the reference flax sample and b) the Verticillium wilt sample. The colour scale gives the related indentation modulus in GPa; c) Distribution of the modulus for the reference and the Verticillium wilt flax samples.

Figure 5. a) Detailed view of fibre cross section AFM measurements from **Figure 4b**. The scale on the left provides the related modulus in GPa. The orange zones show an example of the area used to calculate the mean fibre modulus at 15.85 GPa; c) Evolution of the modulus obtained across the profile shown by the white arrow in the image b).

Figure 6. Transversal SEM observations of elementary flax fibres of a) the reference sample and b) the V. dahliae sample.

Figure 7. Number of *V. dahliae* CAZymes (cellulases, hemicellulases and pectinases) predicted to be secreted. The CAZymes secreted were sorted by class (GH, AA, CE, PL) according to the CAZy classification. GH, glycoside hydrolases; AA, auxiliary activity enzymes; CE, carbohydrate esterases; PL, polysaccharide lyases. The list of CAZymes (sub)families is provided in Table 3.

Table captions

Table 1. Tensile mechanical properties of the reference and Verticillium wilt elementary flax fibre samples.

Table 2. Biochemical composition of the reference and Verticillium wilt flax fibre samples.

Table 3. List of *V. dahliae* CAZymes encoded by the genome and predicted to be secreted. CAZymes are listed with an indication of their family (and subfamily when available), their number, their putative activity and the polysaccharide predicted to be targeted.

Figure 1. Longitudinal SEM observations of a) raw infected flax stems b, d) the reference flax fibre sample, and of c, e) the *V. dahliae* flax fibre sample at different scales.

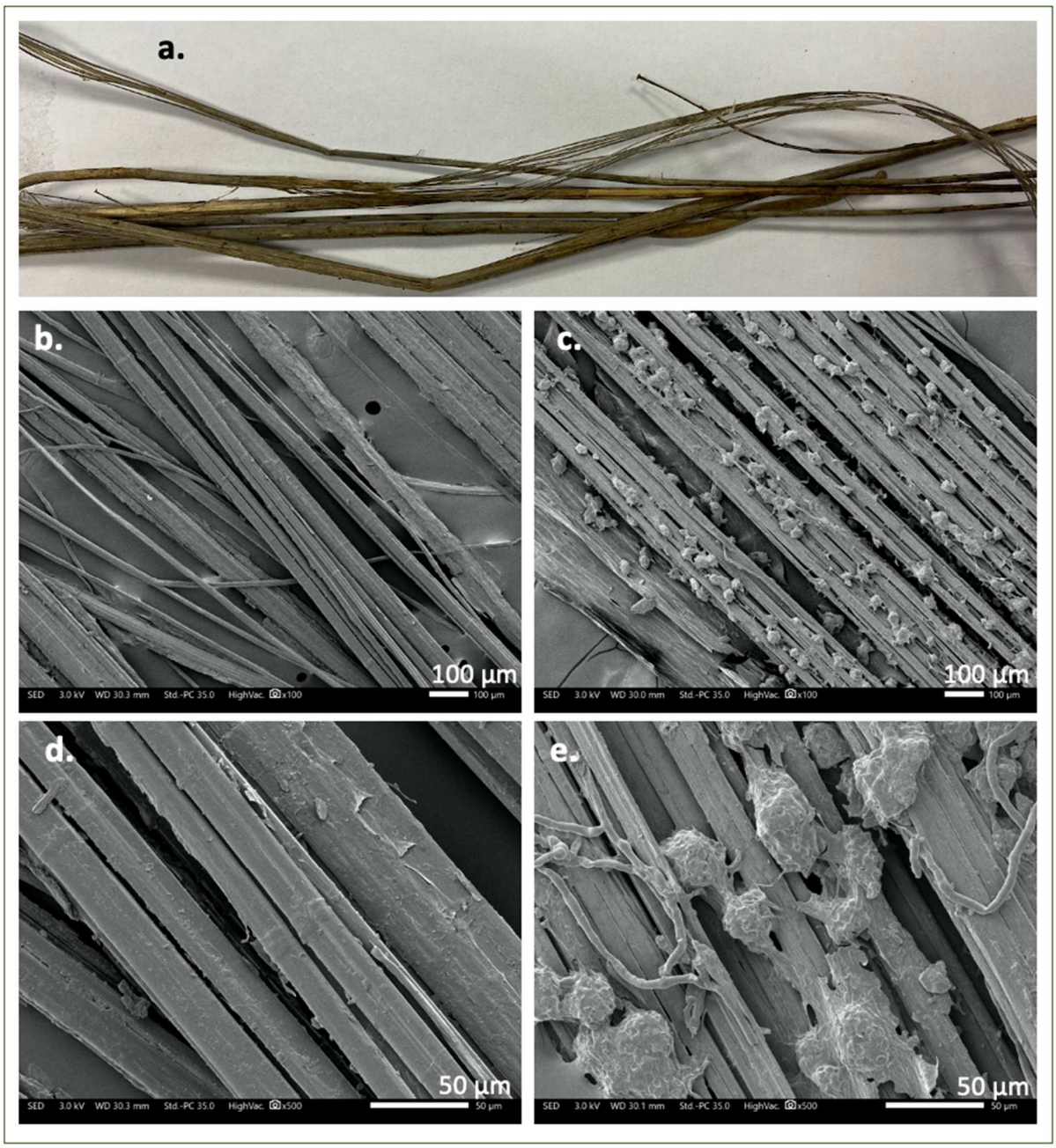

Figure 2. Longitudinal SEM observations of *V. dahliae* flax fibres showing a) microcracks in the cell wall and b) a rugous surface.

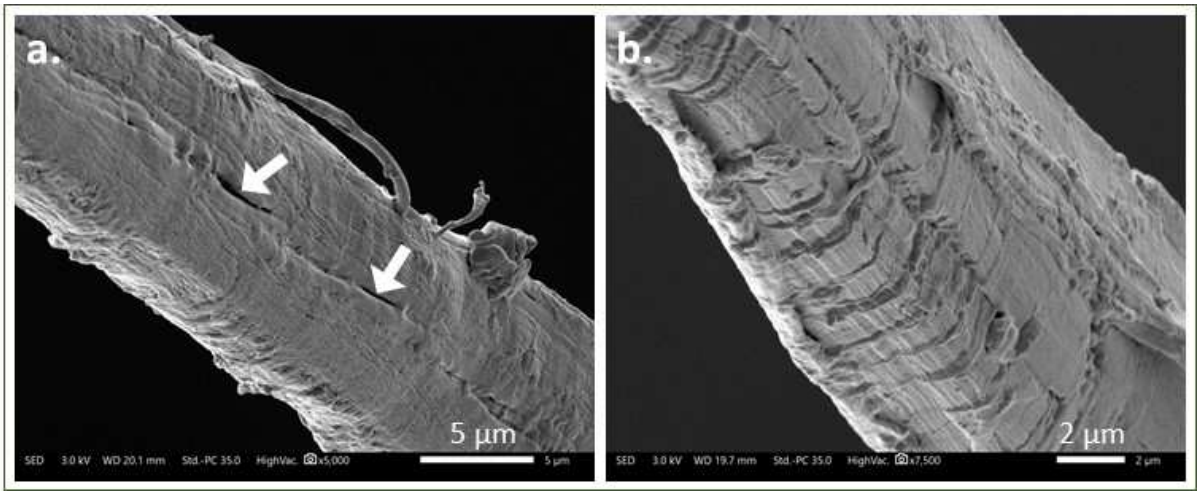

Figure 3. Cumulative probability of the strength at break of the reference and *V. dahliae* elementary flax fibre samples.

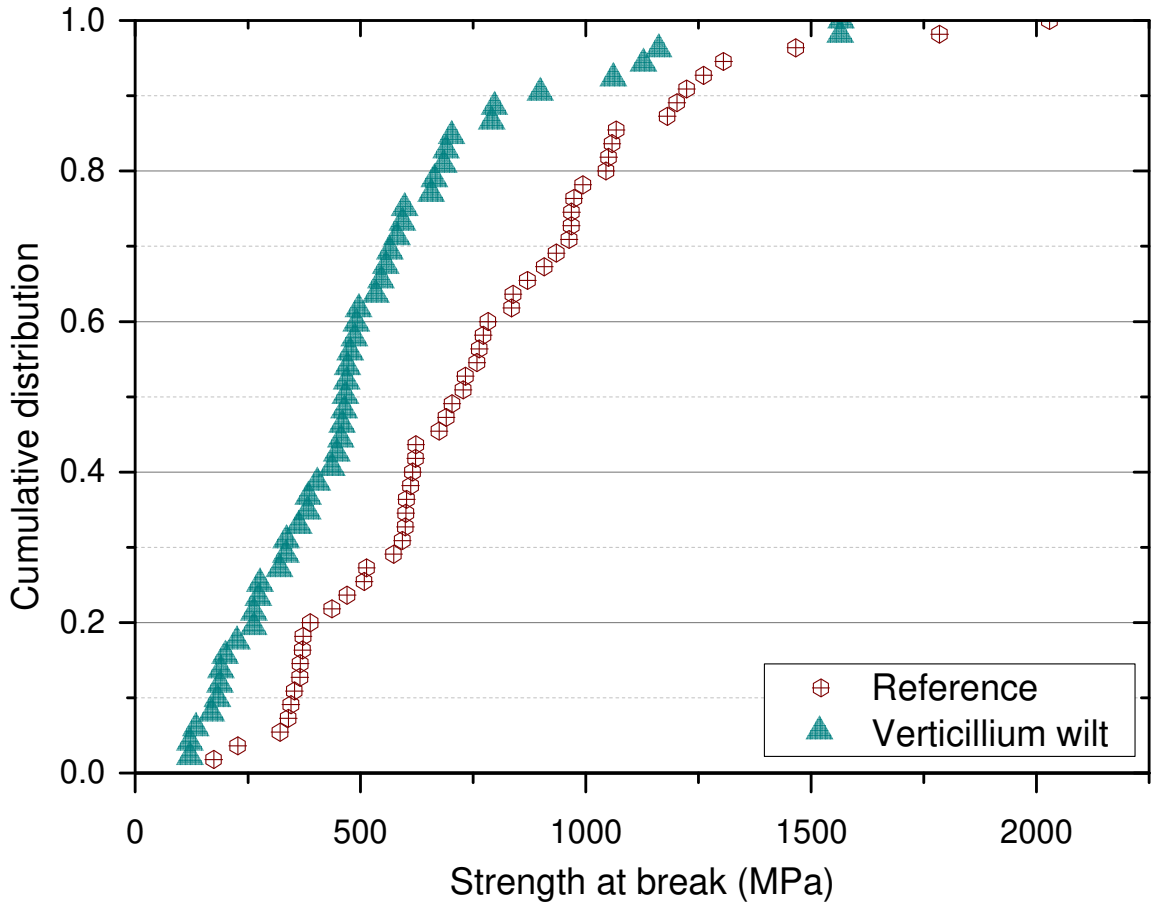

Figure 4. AFM measurements of a) the reference flax sample and b) the Verticillium wilt sample. The colour scale gives the related indentation modulus in GPa; c) Distribution of the modulus for the reference and the Verticillium wilt flax samples.

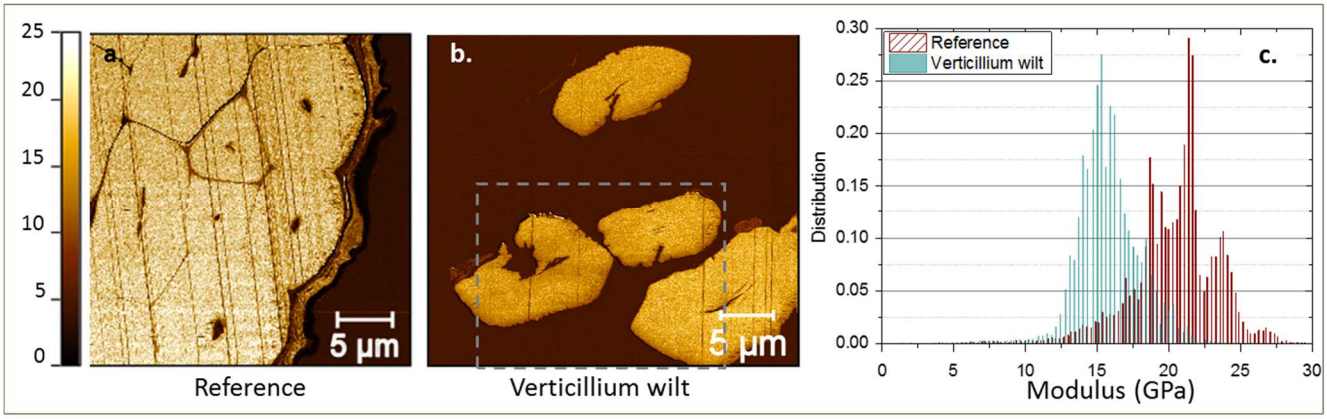

Figure 5. a) Detailed view of fibre cross section AFM measurements from **Figure 4b**. The scale on the left provides the related modulus in GPa. The orange zones show an example of the area used to calculate the mean fibre modulus at 15.85 GPa; c) Evolution of the modulus obtained across the profile shown by the white arrow in the image b).

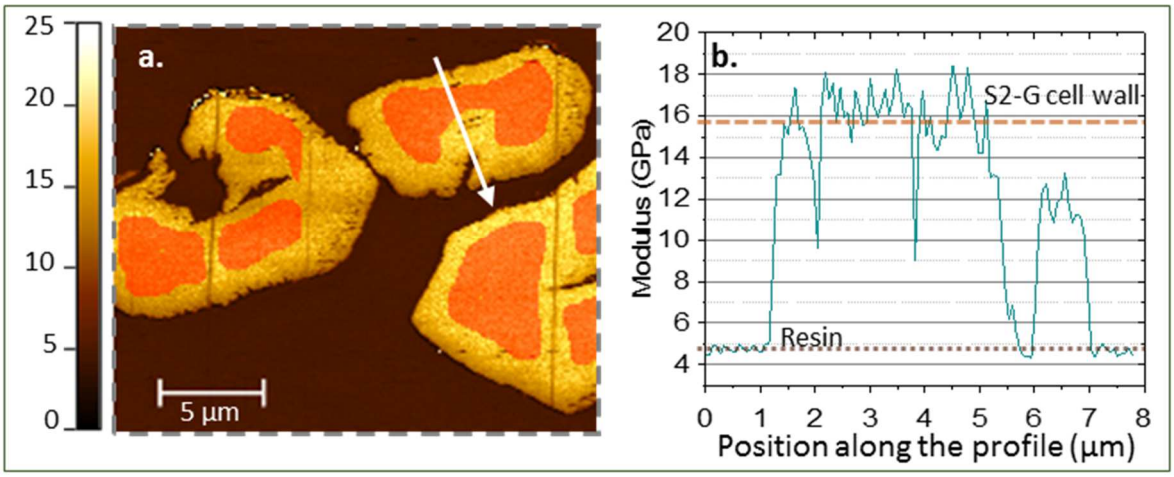

Figure 6. Transversal SEM observations of elementary flax fibres of a) the reference sample and b) the Verticillium wilt sample.

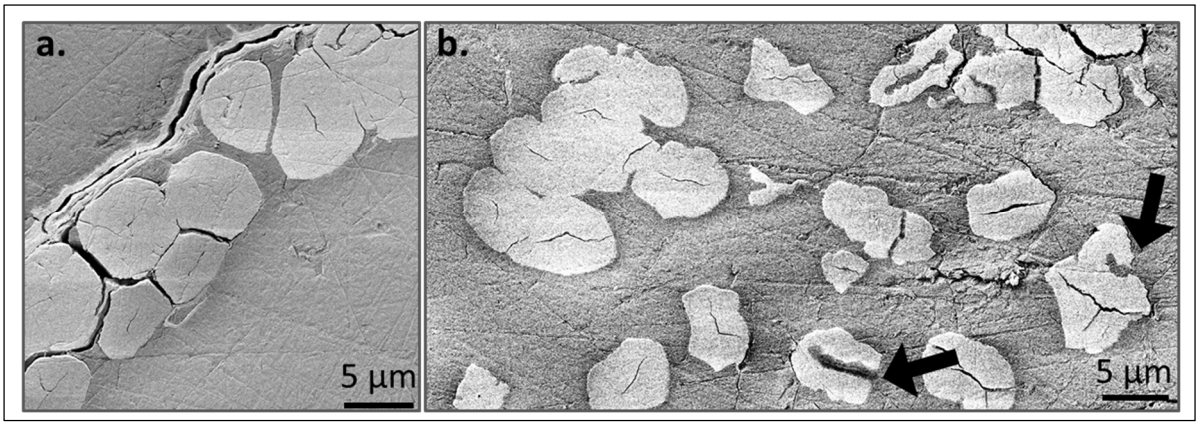

Figure 7. Number of V. dahliae CAZymes (cellulases, hemicellulases and pectinases) predicted to be secreted. The CAZymes secreted were sorted by class (GH, AA, CE, PL) according to the CAZy classification. GH, glycoside hydrolases; AA, auxiliary activity enzymes; CE, carbohydrate esterases; PL, polysaccharide lyases. The list of CAZymes (sub)families is provided in Table 3.

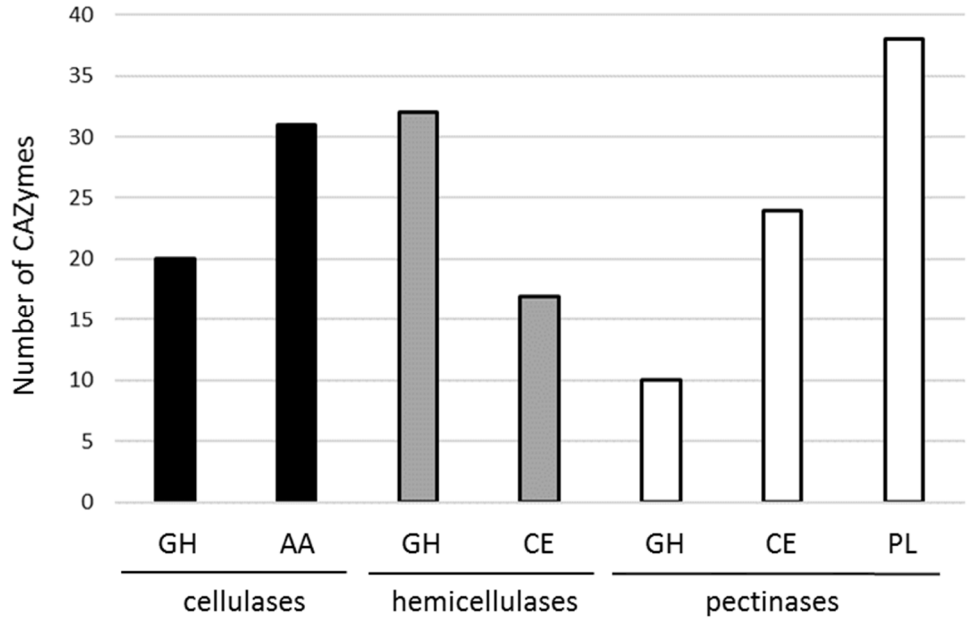

Table 1. Tensile mechanical properties of the reference and Verticillium wilt elementary flax fibre samples.

Sample	**Number of samples**	**Diameter** *(µm)*	**Tangent modulus** *(GPa)*	**Strength at break** *(MPa)*	**Strain at break** *(%)*
Reference	55	15.2	43.6	773	2.09
SD		*3.13*	*17.0*	*374*	*0.59*
Verticillium wilt	52	16.2	34.9	522	1.78
SD		*3.39*	*16.0*	*322*	*0.69*

Table 2. Biochemical composition of the reference and Verticillium wilt flax fibre samples.

Biochemical composition	**Reference**		**Verticillium wilt**	
(% of dry mass)	Mean	*SD*	Mean	*SD*
Fucose	0.04	*0.03*	0.06	*0.01*
Arabinose	1.13	*0.28*	0.98	*0.11*
Rhamnose	0.74	*0.06*	0.72	*0.02*
Galactose	4.37	*0.33*	4.52	*0.03*
Xylose	0.85	*0.18*	1.17	*0.14*
Mannose	4.27	*0.28*	5.22	*0.01*
Galacturonic Acid	0.50	*0.01*	0.49	*0.01*
Glucoronic Acid	0.16	*0.26*	0.18	*0.04*
Glucose	69.79	*1.01*	65.14	*4.19*
Lignin	2.96	*0.08*	3.80	*0.02*

Table 3. List of *V. dahliae* CAZymes encoded by the genome and predicted to be secreted. CAZymes are listed with an indication of their family (and subfamily when available), their number, their putative activity and the polysaccharide predicted to be targeted.

CAZy (sub)Family and module associated	**Number of enzymes predicted to be secreted per family**	**Putative activity**	**Polysaccharide targeted**
AA9	20	Lytic polysaccharide monooxygenase	cellulose
AA9-CBM1	4	Lytic polysaccharide monooxygenase	cellulose
AA16	2	Lytic polysaccharide monooxygenase	cellulose

AA7	2	Glucooligosaccharide oxidase	cellulose
AA8-AA12	1	Pyrroloquinoline quinone-dependent oxidoreductase	cellulose
AA8-AA3_1	1	Cellobiose dehydrogenase	cellulose
AA8-AA3_1-CBM1	1	Cellobiose dehydrogenase	cellulose
CBM1-GH5_4	1	Endo-glucanase	cellulose
CBM1-GH5_5	1	Endo-glucanase	cellulose
CBM1-GH6	1	Endo-glucanase	cellulose
GH6	3	Endo-glucanase	cellulose
GH7	3	Cellobiohydrolase	cellulose
GH7-CBM1	3	Cellobiohydrolase	cellulose
GH12	3	Endo-glucanase	cellulose
GH12-CBM1	1	Endo-glucanase	cellulose
GH45	1	Endo-glucanase	cellulose
GH45-CBM1	1	Endo-glucanase	cellulose
GH131	1	Endo-glucanase	cellulose
GH131-CBM1	1	Endo-glucanase	cellulose
GH5_7	3	Endo-mannanase	hemicellulose
GH5_7-CBM1	1	Endo-mannanase	hemicellulose
CBM1-GH5_7	1	Endo-mannanase	hemicellulose
GH10	2	Endo-xylanase	hemicellulose
GH10-CBM1	1	Endo-xylanase	hemicellulose
GH11	5	Endo-xylanase	hemicellulose
GH11-CBM1	1	Endo-xylanase	hemicellulose
GH27	2	Galactosidase	hemicellulose
GH27-CBM35	1	Galactosidase	hemicellulose
GH43_13	2	Arabinofuranosidase	hemicellulose
GH43_21	1	Arabinofuranosidase	hemicellulose
GH43_22-GH43_34	1	Arabinofuranosidase	hemicellulose
GH43_26	1	Arabinofuranosidase	hemicellulose
GH43_26-CBM42	1	Arabinofuranosidase	hemicellulose
GH43_29	1	Arabinofuranosidase	hemicellulose
GH43_30	1	Galactofuranosidase	hemicellulose
GH43_36	1	Arabinofuranosidase	hemicellulose
GH43-CBM1	1	Arabinofuranosidase	hemicellulose
CBM35-GH26	1	Endo-mannanase	hemicellulose
GH51	1	Arabinofuranosidase	hemicellulose
GH54-CBM42	1	Arabinofuranosidase	hemicellulose
GH67	1	Glucuronidase	hemicellulose
GH115	1	Glucuronidase	hemicellulose
CE1	4	Acetyl xylan / Feruloyl esterase	hemicellulose
CE1-CBM1	1	Acetyl xylan / Feruloyl esterase	hemicellulose
CE3	4	Acetyl xylan esterase	hemicellulose
CE4	4	Acetyl xylan esterase	hemicellulose
CBM1-CE15	1	Methyl glucuronoyl esterase	hemicellulose
CE16	3	Acetyl esterase	hemicellulose
CE4	1	Acetyl xylan esterase	pectin

CE5	13	Acetyl xylan esterase / cutinase	pectin
CE5-CBM1	1	Acetyl xylan esterase / cutinase	pectin
CE8	4	Pectin methylesterase	pectin
$(CE8)_5$	1	Pectin methylesterase	pectin
CE12	4	Pectin acetylesterase	pectin
GH43_24-CBM35	1	Galactanase	pectin
GH53	1	Endo-galactanase	pectin
GH78	3	Rhamnosidase	pectin
GH93	1	Exo-arabinanase	pectin
GH105	3	Rhamnogalacturonyl hydrolase	pectin
GH146	1	Arabinofuranosidase	pectin
PL1	3	Pectate lyase	pectin
PL1_2	2	Pectate lyase	pectin
PL1_4	5	Pectate lyase	pectin
PL1_4-CBM1	1	Pectate lyase	pectin
PL1_7	4	Pectate lyase	pectin
PL1_9	1	Pectate lyase	pectin
PL1_10	1	Pectate lyase	pectin
PL3_2	10	Pectate lyase	pectin
CBM1-PL3_2	1	Pectate lyase	pectin
PL4	2	Rhamnogalacturonan endolyase	pectin
PL4_1	1	Rhamnogalacturonan endolyase	pectin
PL4_3	3	Rhamnogalacturonan endolyase	pectin
PL9_3	2	Pectate lyase	pectin
PL26	1	Rhamnogalacturonan exolyase	pectin
PL42	1	Rhamnohydrolase	pectin